Supplement of Clim. Past, 22, 1037–1055, 2026
https://doi.org/10.5194/cp-22-1037-2026-supplement

Climate of the Past
Open Access
EGU

Supplement of

A multimillennial Alpine ice core chronology synchronized with an accurately dated Arctic Pb record

Paolo Gabrielli et al.

Correspondence to: Paolo Gabrielli (paologabrielli@hotmail.com), Theo M. Jenk (theo.jenk@psi.ch), and Carlo Barbante (barbante@unive.it)

S1: Structure of the TC2016 chronology

The initial chronology, TC2016 (Gabrielli et al., 2016), was developed by utilizing a common depth scale for Alto dell'Ortles cores #1, #2, and #3, using core #2 depth as a reference. Depth alignment of core #2 with #1 and with #3 was accomplished by matching common features in their $\delta^{18}O$ records (17 between #2 and #1, 14 between #2 and #3) (see Fig. 10 in Gabrielli et al., 2016). This allowed the transfer of time markers in the cores to a common depth scale. Because of the lower resolution of the $\delta^{18}O$ record in core #3, only two match features, or "tie points", could be established between cores #3 and #2 below 60 m depth. However, we realized later that this resulted in a depth misalignment of only few tens of cm, which nevertheless resulted in a significant time lag (up to ~300 years) between the 3 cores. This mismatch in depth and time became apparent by comparing two new high resolution Pb concentration records from cores #1 and #3 with TC2016 (see main text), showing a much larger Pb variability below 60 m depth, compared to the variability in $\delta^{18}O$.

S2: Methodologies adopted to determine Pb

Two high resolution Pb concentration records were independently determined in Alto dell'Ortles cores #1 and #3 by discrete Inductively Coupled Plasma Mass Spectrometry (ICP-MS) and continuous flow analysis (CFA) ICP-Sector Field MS (ICP-SFMS) at the University of Venice (UV) and at the Ohio State University (OSU), respectively (Gabrieli, 2008; Gabrieli and Barbante, 2014).

At OSU a melter system identical to the one developed at UV (Gabrieli, 2008) was adopted to continuously melt ice sticks that were cut from core #3 with a cross section of 3.2 x 3.2 cm. Online acidification was performed using ultraclean HNO_3 (Optima, Thermofisher) to obtain a final acid concentration of 1% v/v. In this way, acid leaching before sample introduction in the ICP lasted 1-2 minutes only. At UV an identical melter system and a fraction collector were used to melt ice sticks cut from core #1 to fill with meltwater 30 mL narrow mouth LDPE bottles (Nalgene). In this case HNO_3 (Optima, Thermofisher) acidification (1 % v/v) of the aliquots was performed the day before the analyses (12-24 hours of leaching time). For both methodologies at OSU and UV the Pb procedural blanks were estimated by melting artificial ice core sticks made of ultrapure deionized water and were found below the limit of detection (1 pg/g). Accuracy and precision were estimated using a spiked deionized water solution of 1 ng/g of Pb and were within 5-8% and 2-3% after 10 replicates, respectively.

The observed differences in Pb concentrations between cores #1 and #3 (Fig. 2) are most likely related to the different acid leaching time for the continuous flow analysis (CFA; using online acidification; core #3) and discrete analysis (adopting pre-acidification of aliquots during sample preparation; core #1). Trace metal concentration differences due to acid leaching are often related to method specific acidification of the samples prior the analyses. This depends on acid concentration, acidification time (e.g., Uglietti et al., 2014; Rhodes et al., 2011, Arienzo et al. 2018) and, as we demonstrated in Uglietti et al. (2014), also on the chemical/mineralogical characteristics of the various samples collected from different study sites. According to a previous test with one single ice sample from the same Alto dell'Ortles ice cores (Uglietti et al. 2014), Pb concentration may not seem to be affected by acid leaching time. However, in that study changes were investigated for acidification times between 24 h and 43 days, not covering the short acidification timescale typical of continuous flow analysis

(1-2 minutes; core #3 analyses) and discrete analysis (less than 24 hours; core #1 analyses). In a more recent manuscript, these shorter timescales, from minutes to a few hours, were investigated (1.5-250 minutes) for alpine ice core samples of similar concentration as analysed in this study (Münster et al., 2025). While these results cannot be automatically generalized and extended to other drilling sites, they do show a 2-to-3-fold increase in the measured Pb concentration over that short time range which would explain the observed difference in absolute Pb concentration between Alto dell'Ortles cores #1 and #3 due to differences in the method dependent acidification times applied.

Additionally, Pb concentration differences are likely larger at low concentration levels where Pb leaching from mineral dust particles becomes relatively more important. Another factor is the dust size and particle surface (roughness), with particularly the larger surfaces likely leading to enhanced leaching. In any case, different acidification methods do not affect general trends and the main features of the Pb records (maxima, minima, Pb variations) used for wiggle matching in this study. This is indicated by the excellent match of the overlayed records, both visually (lower panel of Fig. 2 in the main text) and statistically ($r = 0.91$, $p < 0.01$). A potential slight depth misalignment caused by the different spatial resolution obtained by using either analytical method (~ 0.2 cm and ~ 4 cm in the cores #3 and #1, respectively) is negligible with respect to the final temporal uncertainty.

S3: Example for the synchronization of ncPb records from Alto dell'Ortles and the Arctic (AN), and discussion of the Alto dell'Ortles record for the industrial period

Details and exact procedures applied for synchronization the ncPb records are provided in sect. 5 in the main text. For illustration, we here provided a practical example of the applied tie-point selection and resulting synchronization. Before synchronizing CP2025/1 with AN, the oldest peak in Pb concentration in the Alto dell'Ortles cores (sea peak 3 in Fig. S4) was assigned to an age of 510-320 BCE (1σ uncertainty range of the peak in CP2025/1). After synchronization, that peak is shifted to an age of 205-145 BCE (1σ uncertainty range in CP2025/2). In this case, the applied shift from CP2025/1 to CP2025/2 was consistent within their 2-sigma range. In another instance, a feature of elevated concentrations (indicated with X in Fig. S4), which however was not characterized by a distinct peak maximum, was initially dated to span from 350 ± 110 BCE to 515 ± 270 CE (CP2025/1). In the absence of a clear maxima (or "mid-point") to be used as a well-defined tie-point for X, the minima 1 and 2 shown in Fig. S4 could, in this case, be used instead. After synchronization (i.e., on CP2025/2), the spanned time interval of this feature (X), although not being defined by assigning a specific date to a maximum of it, resulted with 65 ± 30 BCE to 245 ± 50 CE. It is noteworthy that when finally displayed on CP2025/2, the Alto dell' Ortles ncPb record shows remarkable similarity with the signal in AN for the covered common time of the Roman period (from 200 BCE to 300 CE; Fig S4 panel c). This is also true for the comparison from 500 BCE to 300 CE with a more recent Arctic Pb ice core composite from McConnell et al., 2025 (Fig. S4 panel d; three ice cores, with AN being one of them). Specifically, also the resulting shape and structure of the feature X, covering the period of the Roman Empire (around 10 BCE to 200 CE according to the dating of the Arctic composite), shows remarkable similarity (panel d), even though there was no tie-point selected within this

time interval (interesting also to note that the level of agreement/disagreement with the composite is about the same for Ortles and AN).

Although wiggle matching was not applied to the most recent ~260 years of the record (1755–2012 CE; see sect. 5 in the main manuscript), a brief discussion of the industrial-period section of the record is provided here. From a geochemical point of view, a peculiar observation is that the ncPb concentrations in the Alto dell'Ortles core at around 600 CE and 1400 CE (based on the independent ^{14}C dates) are higher than the recorded concentrations in the industrial period. This is in contrast with the published Pb ice core records from Greenland (McConnell et al., 2019) and the Alps (Gabrieli et al., 2014; Preunkert et al., 2019). Here we preliminarily provide two possible explanations. First, the interplay between ancient/regional Tyrolean mining Pb sources (von Scheffer et al. 2024 and references therein) with high emission factors and modern/distant sources might partly explain the observed ncPb trends in the Alto dell'Ortles ice core. In fact, Tyrolean and continental sources of atmospheric ncPb are likely to modulate the amplitude of ncPb concentrations at the high altitude Central European drilling site of Alto dell'Ortles. In this way, Mt. Ortles is likely strongly influenced by these two kinds of distinct contributions whereas these same sources would affect with a different intensity the more distant Arctic drilling site of AN. A second possible explanation relates to the fact that the Alto dell'Ortles drilling site is temperate in the upper firn part (down to 30 m depth; Gabrielli et al., 2012) and a depletion in the Pb signal from post depositional effects, i.e., from melt-water percolation, cannot be excluded (see e.g., Huber et al., 2024; and Avak et al., 2018, estimating up to 50% loss for the Pb signal in temperate firn).

S4: Colle Gnifetti ice core – timescale and ncPb record

The glacier on Colle Gnifetti (Mt. Rosa, Western Alps) currently contains the oldest ice found in the Alps with a ^{14}C confirmed age (>15000 years; Jenk et al., 2009). Colle Gnifetti Pb records were previously published by Schwikowski et al. (2004) and by Gabrieli and Barbante (2014). The chronology presented in the latter 2014 publication was based on the dating by Jenk et al. (2009). Here, we take advantage of a revised dating of the Colle Gnifetti ice core (CG03B) applied to the record from Gabrieli and Barbante (2014. As shown in Fig. S5, compared to the timescale published by Jenk et al. (2009), CG03B includes revisions in the counting of annual layers (ALC) based on additional reference horizons of historical Sahara dust layers (SDL) and volcanic layers (VL) (Sigl et al., 2018), as well as two additional ^{14}C-dates (Sigl et al., 2009). Thus, the CG03B timescale is based on ALC (from 1763 to 2003 CE), anchored by a distinct ^{3}H peak, historical SDL and VL, and independently confirmed by absolute dating with ^{210}Pb activity (Jenk et al., 2009; Sigl et al., 2018). Before 1763 CE ages are modeled as an exponential equation constrained by ^{14}C-dates from the measured water insoluble organic carbon (WIOC-14) fraction of carbonaceous particles (Jenk et al., 2009; Sigl et al., 2009), assuming steady-state conditions and using a 1D ice flow model (2-parameter model, 2-p model) (Jenk et al., 2009). The CG03B timescale has a relatively small uncertainty back to 1763 CE (up to a maximum of around ± 5 years) that increases significantly to ~ ± 250 years at the beginning of the record at ~ 350 CE. CG03B was previously used in Sigl et al. (2018) and Brugger et al. (2021).

In Fig. S6, a comparison of the independently dated Colle Gnifetti non-crustal Pb (ncPb) concentration record with the Alto dell'Ortles record on its revised time scale (CP2025/2) is provided for the part of the CG record dated with still

reasonably high accuracy and precision (see above). For the Colle Gnifetti core, the ncPb record was obtained from Pb concentrations corrected for mineral dust contribution using the average crustal Pb/Ti ratio (0.00545 obtained from Wedepohl, 1995). A similar comparison with the Arctic record from AN – which was used as the reference in terms of its chronology for the new dating of the Alto dell'Ortles cores by synchronization (see also main text) – is shown in Fig. S7, here for the entire length of the records.

S5: Dansgaard-Johnsen (DJ) model framework

To understand our approach outlined in the main text, it is important to recognize that under the assumed steady-state conditions at the drill site, net annual snow accumulation (b, which in the accumulation zone equals the mass balance at that point; Cogley et al., 2011) and v_x along the glacier vertical profile are closely related. For reasons of mass conservation, if the amount of accumulated snow is not to increase the thickness of the glacier at that point, the same mass quantity must be removed from the ice column below. In more glaciological terms, the accumulated snow needs to be balanced by the horizontal strain and, due to the incompressibility of ice, the corresponding vertical strain rates (note the reduction to 1D, i.e., to the vertical axis). These fundamental principles are governed by the equation of continuity which, if integrated over the ice thickness, can also be written to relate to time and density (e.g., Whillans, 1977). In the DJ model, which considers these principles, the cumulative vertical strain of a layer at a certain depth over time (i.e., the total thinning) is related to the value of h. The DJ model accounts for the importance of density by using m w.e. as unit of length. This is essential, because in the firn section of the vertical column a substantial part of the horizontal stress will not cause deformation (i.e. the thinning governed by the model related to the incompressibility of ice), but instead enhances firn compaction by internal creep.

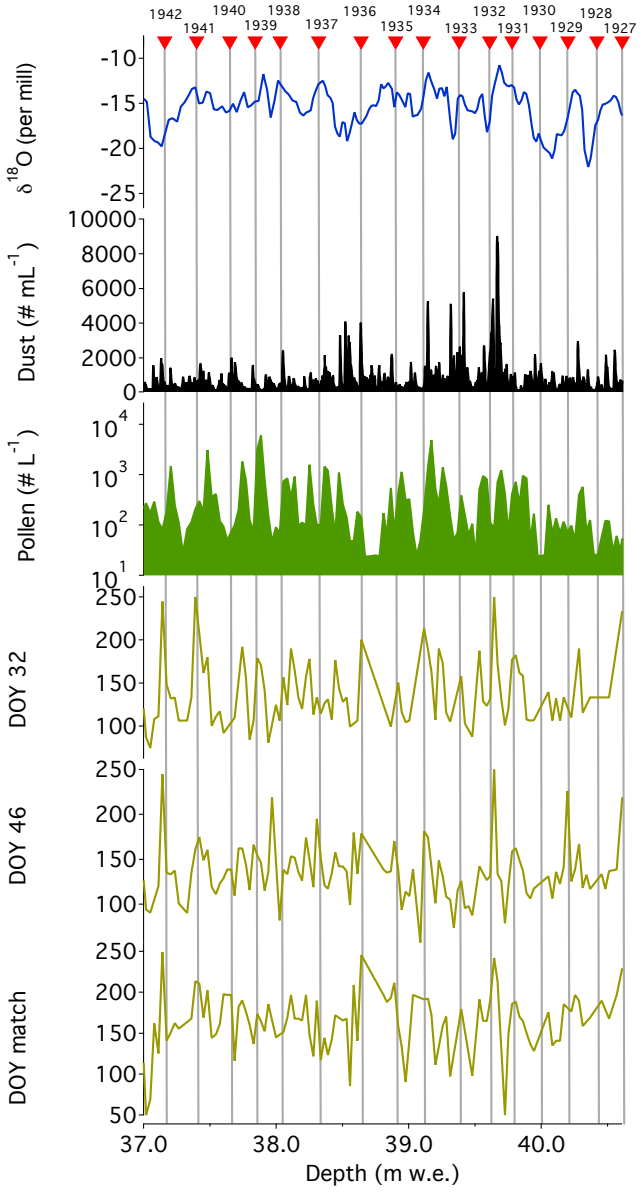

Figure S1: Annual layers between 37 and 41 m water equivalent (w.e.) in core #1 as shown by $\delta^{18}O$, dust and pollen concentrations, Day-Of-the-Year (DOY) 32 and 46 and DOY depth-to-day match (see main text).

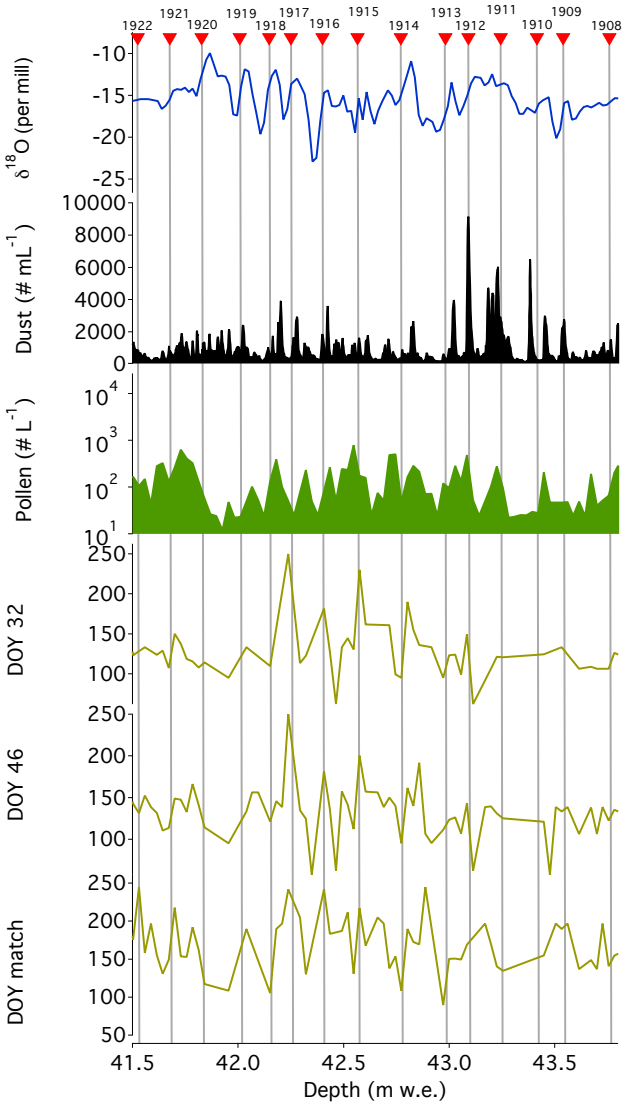

5 Figure S2: Annual layers between 41.5 and 43.5 m water equivalent (w.e.) in core #1 as shown by $\delta^{18}O$, dust and pollen concentrations, Day-Of-the-Year (DOY) 32 and 46 and DOY depth-to-day match (see main text).

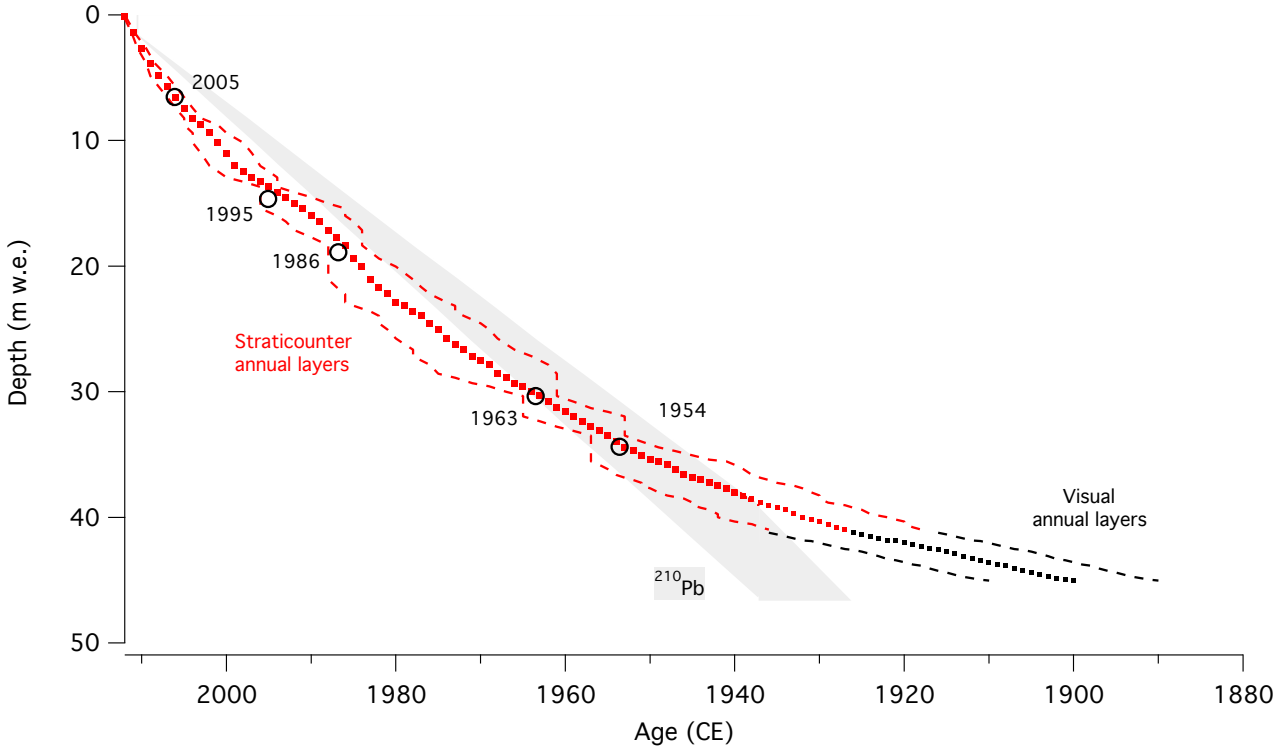

Figure S3: Comparison of the different time markers obtained in the shallow (recent) part of the Alto dell'Ortles cores. StratiCounter annual layer automatic counting (red dots; within 95% uncertainty) are superimposed on 5 fixed time markers (open circles; see also Table 3). ^{210}Pb ages from the TC2016 chronology are shown with uncertainty range (grey area; from Gabrielli et al., 2016). Annual layers determined by visual counting (black dots within an assumed 10 year uncertainty).

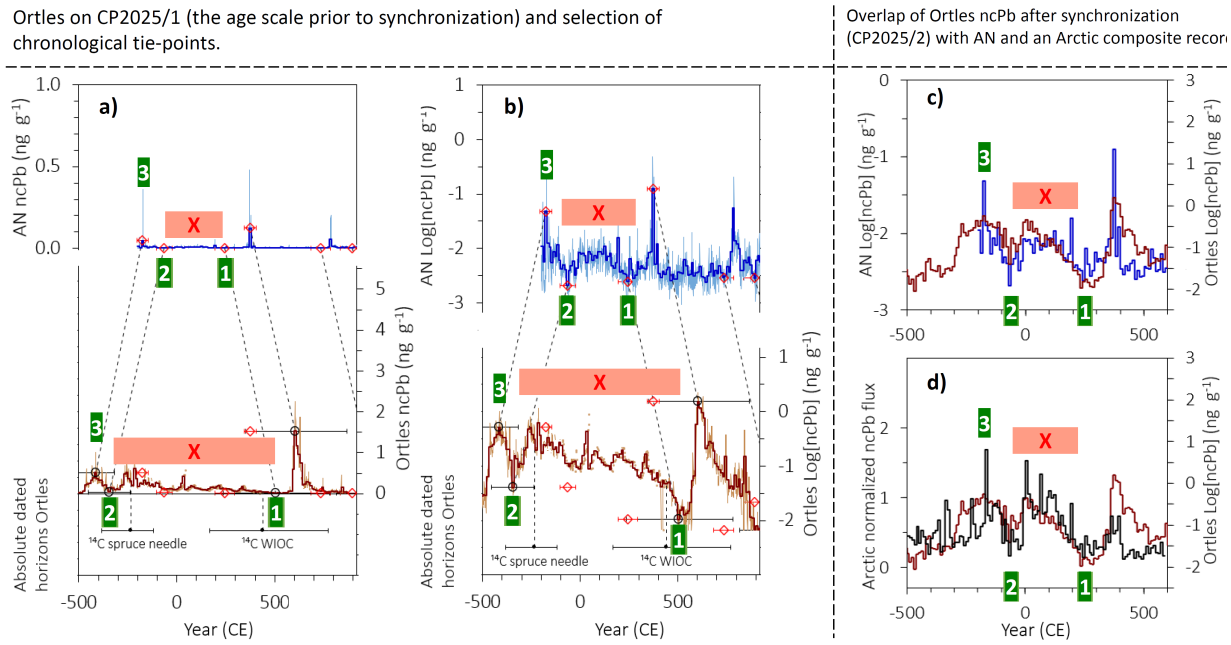

Figure S4: Examples for synchronization by wiggle matching of the ncPb Alto dell'Ortles with the Arctic record from AN (McConnell et al., 2019), including comparison to a more recent Arctic composite record (McConnell et al., 2025). Panels a) and b) show time sections extracted from Fig. 6 in the main manuscript. Panel c) is an adaptation of Fig. 8 in the main manuscript. Panel d) is the same as panel c but using the normalized ncPb flux from a composite of three Arctic ice cores (McConnell et al., 2025, Fig. 1 therein). All data are consistently displayed as 10-year averages (see sect. 5 in the main manuscript).

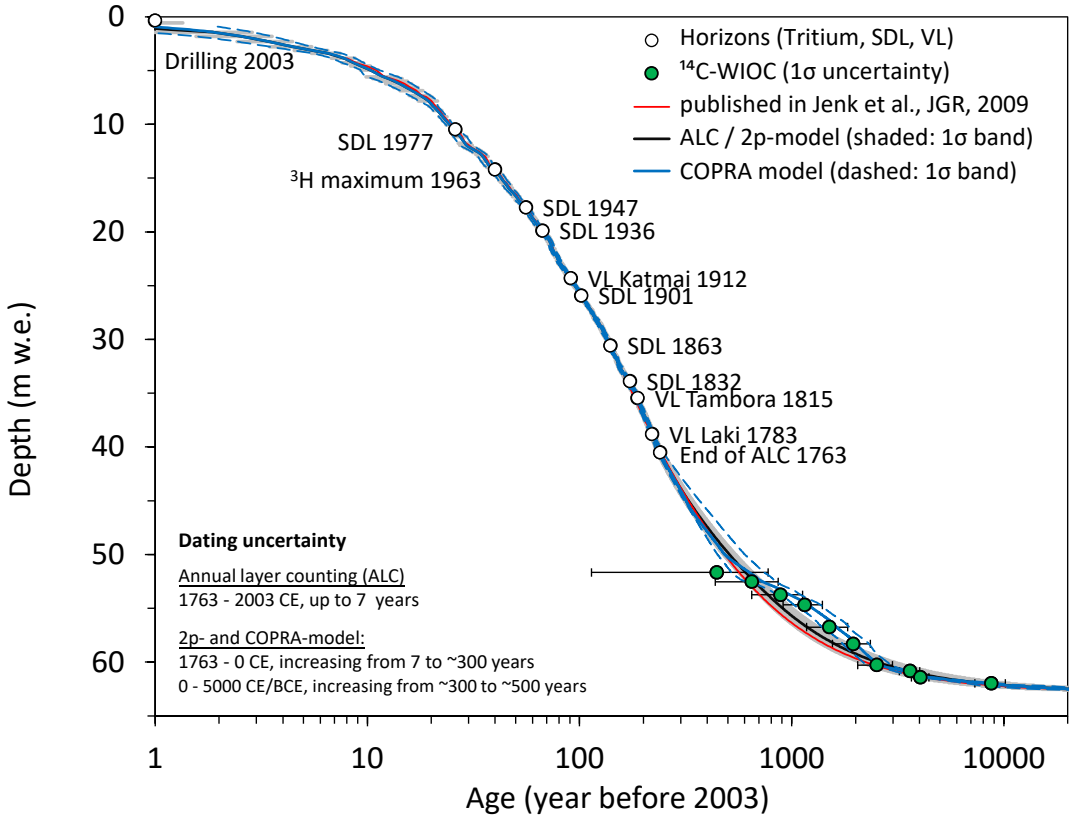

Figure S5: Dating of the Colle Gnifetti ice core (CG03B). Note the logarithmic age axis. This is a revised dating of Jenk et al. (2009) (red dashed line). This update also includes a revised counting of annual layers (ALC) based on additional reference horizons of historical Sahara dust layers (SDL) and volcanic layers (VL) (Sigl et al., 2018), as well as two additional ^{14}C-dates (Sigl et al., 2009). For details see section S4 in the Supplement. Additionally shown here is the age scale derive by using the COPRA model in an exact same approach as used for the Alto dell'Ortles cores dating and using the time horizons indicated (blue lines).

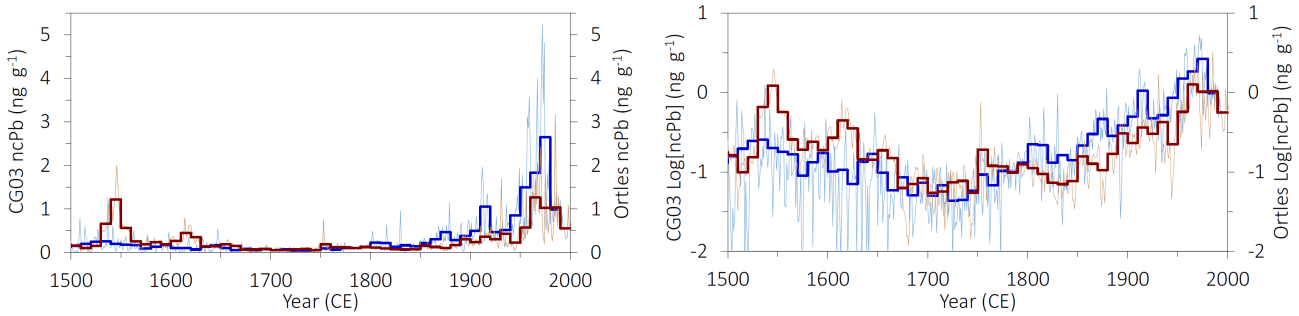

Figure S6: Comparison of the non-crustal Pb concentrations (ncPb) from Alto dell'Ortles #3 on CP2025/2 (Ortles; dark red) with the record from the Colle Gnifetti ice core (CG03; blue) back to 1500 CE. Thin and thick lines show annual and 10-year averages, respectively. Same for both panels, except for ncPb concentrations being plotted on a logarithmic scale on the right panel.

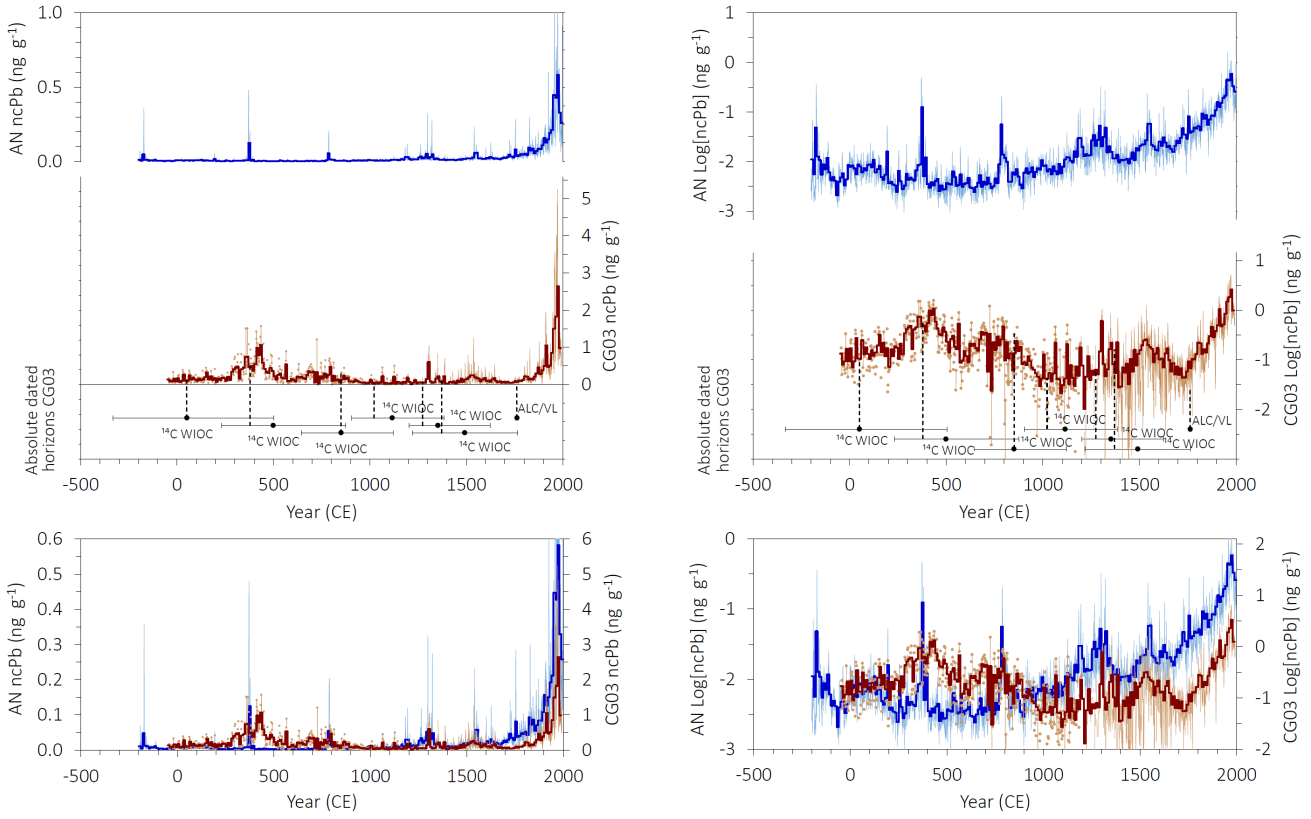

Figure S7: Comparison of the non-crustal Pb concentrations (ncPb) from the Colle Gnifetti ice core (CG03; dark red) (Jenk et al., 2009)(Sigl et al., 2018) with the record from Akademii Nauk (AN; blue) (McConnell et al., 2019). Thin and thick lines show annual and 10-year averages, respectively. Absolute ages from ^{14}C dating (or ALC/VL) are shown at the bottom (dots indicate the μ-age and error bars the 1σ range), with the thick dashed line connecting to the record for visualizing the time horizons used to construct the CG03B time scale with COPRA (see section S4 in the Supplement and Fig. S2). Same for both panels, except for ncPb concentrations being plotted on a logarithmic scale on the right panel. Bottom two panels with the ncPb records shown in the upper panels being overlayed to facilitate visual comparison.

Table S1: Details on pollen records used in Straticounter to obtain annual layer counting.

Pollen record	Ortles pollen types included	Type of data and method	Dataset in Zenodo
Depth-to-day match	*Abies; Acer; Alnus; Alnus viridis; Ambrosia; Artemisia; Asteraceae; Betula; Calluna vulgaris; Campanula;* Cannabaceae; *Carpinus betulus*; Caryophyllaceae; *Castanea sativa; Cedrus;* Chenopodiaceae T.*;* Cichoriaceae; *Corylus avellana;* Crassulaceae; Cruciferae*;* Cyperaceae; *Equisetum;* Ericaceae; *Fagus; Fraxinus excelsior; Fraxinus ornus;* Gramineae; H*elianthemum; Juglans; Juniperus; Larix;* Liliaceae T.*; Lotus T.;* Malvaceae; Monolete Spores; *Ostrya T.;* Papilionaceae; *Picea; Pinus; Pinus cembra; Plantago; Plantago alpina T.; Plantago coronopus; Plantago lanceol. T.; Plantago major; Plantago major T.;* Polygonaceae; *Polygonum bist. T.; Quercus robur T.;* Ranunculaceae; *Rhinanthus; Rosaceae;* Rubiaceae; *Rumex acetosa T.; Rumex acetosella; Rumex T.; Salix; Saxifraga granulata T.;* Scrophulariaceae; *Senecio T.; Silene; Sorbus T.; Taxus baccata; Thalictrum; Tilia*; Trilete Spores; *Ulmus;* Umbelliferae; *Urtica; Veronica*.	This record was obtained by comparison of Ortles pollen samples with 10 years of daily airborne pollen measurements from the nearby Bolzano air monitoring station (Italy). Nomenclature of the pollen types observed and their significance for plant species are consistent with those used in the European Pollen Database. The comparison method uses presence (1)/ absence (0) of the pollen types. Calculations follow Festi et al. (2017). In brief, Ortles ice samples are characterised by their depth and pollen spectra, while Bolzano pollen monitoring samples are characterised by their pollen spectra and accurate temporal data. By finding for an Ortles sample the most similar Bolzano's sample according to their pollen content, we established a direct depth-to-day link. In this way every Ortles sample containing pollen has been dated.	Raw data: https://doi.org/10.5281/zenodo.18384389 Results: https://doi.org/10.5281/zenodo.18384151
DOY (day of the year) 32	1.*Abies*; 2.*Acer*; 3.*Ambrosia*; 4.*Artemisia*; 5.*Betula*; 6.Cannabaceae; 7.*Carpinus betulus*; 8.*Castanea sativa*; 9.*Corylus avellana*; 10.Cyperaceae; 11.Ericaceae; 12. *Fagus*; 13. *Fraxinus excelsior*; 14. *Fraxinus ornus*; 15.*Hedera helix*; 16. *Juglans*; 17. *Larix*; 18.Monolete spores; 19.*Olea*; 20.*Ostrya* T.; 21.Palmae; 22.*Picea*; 23.*Pinus cembra*; 24.*Polygonum*; 25.*Populus*; 26.*Quercus robur* T.; 27.Ranunculaceae; 28.Rubiaceae; 29.*Salix*; 30.*Tilia*; 31.*Ulmus*; 32.*Vitis*	Using a multiple Weighted Averaging (WA) method the pollen deposition day on the ice/snow of the Ortles glacier was calculated (Day of the year, DOY ± SD). WA is used in Correspondence Analysis (CA) proposed by Hill (1974). The dating method is based on pollen count data of 32 taxa from recent decades, determined by the pollen forecast services Bolzano and Obergurgl, and these data are used to determine the age of the ice (in DOY ± SD) based on the pollen composition of the ice/snow sample.	Raw data: https://doi.org/10.5281/zenodo.18384281 Results: https://doi.org/10.5281/zenodo.18384151
DOY (Day of the year) 46	1.*Abies; 2.Acer*; 3. *Alnus*; 4. *Alnus viridis*; 5.*Ambrosia*; 6.*Artemisia*; 7.Asteraceae; 8.*Betula*; 9.Cannabaceae; 10.*Carpinus betulus*; 11.*Castanea sativa*; 12.*Cedrus*; 13.Chenopodiaceae T.; 14.*Corylus avellana*; 15.Cupressaceae; 16.Cyperaceae; 17.Ericaceae; 18.*Fagus*; 19.*Fraxinus excelsior*; 20.*Fraxinus ornus*; 21.*Hedera helix*; 22.*Juglans*; 23.*Larix*; 24.Monolete spores; 25.Moraceae; 26.*Olea*; 27.*Ostrya* T.; 28.Palmae; 29.*Picea*; 30.*Pinus*; 31.*Pinus cembra*; 32.*Plantago*; 33.Poaceae; 34.*Polygonum*; 35.*Populus*; 36.*Quercus robur* T.; 37.Ranunculaceae; 38.Rosaceae; 39.Rubiaceae; 40.*Rumex*; 41.*Salix*; 42.*Tilia*; 43.*Ulmus*; 44.Umbelliferae; 45.Urticaceae; 46.*Vitis*.	Using a multiple Weighted Averaging (WA) method the pollen deposition day on the ice/snow of the Ortles glacier was calculated (Day of the year, DOY ± SD). WA is used in Correspondence Analysis (CA) proposed by Hill (1974). The dating method is based on pollen count data of 46 taxa from recent decades, determined by the pollen forecast services Bolzano and Obergurgl, and these data are used to determine the age of the ice (in DOY ± SD) based on the pollen composition of the ice/snow sample.	Raw data: https://doi.org/10.5281/zenodo.18384281 Results: https://doi.org/10.5281/zenodo.18384151

Table S2: Time markers used for the CP2025/1 timescale construction (part 1).

Depth in core #2 (m w.e.)	Age (yrsb2012)	Age uncertainty (years)	Type of time marker	Used in COPRA model
0.144	0.01	0.1	Annual layer (Straticounter)	✓
1.435	1	0.2	Annual layer (Straticounter)	✓
2.652	2	0.5	Annual layer (Straticounter)	✓
3.843	3	0.5	Annual layer (Straticounter)	✓
4.868	4	1	Annual layer (Straticounter)	✓
5.713	5	1	Annual layer (Straticounter)	✓
6.551	6	1	Annual layer (Straticounter) and 2006 pollen peak	✓
7.404	7	1	Annual layer (Straticounter)	✓
8.217	8	1	Annual layer (Straticounter)	✓
8.761	9	2	Annual layer (Straticounter)	✓
9.407	10	2	Annual layer (Straticounter)	✓
10.182	11	3	Annual layer (Straticounter)	✓
11.022	12	3	Annual layer (Straticounter)	✓
12.017	13	3	Annual layer (Straticounter)	✓
12.457	14	3	Annual layer (Straticounter)	✓
12.931	15	3	Annual layer (Straticounter)	✓
13.268	16	2	Annual layer (Straticounter)	✓
13.687	17	1	Annual layer (Straticounter) and 1995 pollen peak	✓
14.116	18	2	Annual layer (Straticounter)	✓
14.509	19	3	Annual layer (Straticounter)	✓
15.011	20	4	Annual layer (Straticounter)	✓
15.402	21	5	Annual layer (Straticounter)	✓
16.001	22	4	Annual layer (Straticounter)	✓
16.454	23	4	Annual layer (Straticounter)	✓
17.121	24	4	Annual layer (Straticounter)	✓
17.712	25	3	Annual layer (Straticounter)	✓
18.332	26	2	Annual layer (Straticounter) and 1986 Beta peak	✓
19.395	27	3	Annual layer (Straticounter)	✓
20.036	28	4	Annual layer (Straticounter)	✓
21.048	29	5	Annual layer (Straticounter)	✓
21.660	30	5	Annual layer (Straticounter)	✓
22.223	31	5	Annual layer (Straticounter)	✓
22.884	32	6	Annual layer (Straticounter)	✓
23.162	33	6	Annual layer (Straticounter)	✓
23.615	34	5	Annual layer (Straticounter)	✓
23.952	35	5	Annual layer (Straticounter)	✓
24.536	36	6	Annual layer (Straticounter)	✓
25.043	37	6	Annual layer (Straticounter)	✓
25.761	38	6	Annual layer (Straticounter)	✓
26.200	39	6	Annual layer (Straticounter)	✓
26.633	40	6	Annual layer (Straticounter)	✓
27.166	41	7	Annual layer (Straticounter)	✓
27.510	42	7	Annual layer (Straticounter)	✓
27.849	43	7	Annual layer (Straticounter)	✓
28.550	44	7	Annual layer (Straticounter)	✓
28.880	45	6	Annual layer (Straticounter)	✓
29.307	46	5	Annual layer (Straticounter)	✓
29.573	47	4	Annual layer (Straticounter)	✓
29.985	48	3	Annual layer (Straticounter)	✓
30.327	49	2	Annual layer (Straticounter) and 1963 tritium beta peaks	✓
30.802	50	3	Annual layer (Straticounter)	✓
31.295	51	4	Annual layer (Straticounter)	✓
31.599	52	5	Annual layer (Straticounter)	✓
31.966	53	6	Annual layer (Straticounter)	✓
32.334	54	5	Annual layer (Straticounter)	✓
32.775	55	4	Annual layer (Straticounter)	✓
33.118	56	3	Annual layer (Straticounter)	✓
33.496	57	2	Annual layer (Straticounter) and 1955 beta peak	✓
33.964	58	3	Annual layer (Straticounter)	✓
34.427	59	4	Annual layer (Straticounter)	✓
34.710	60	5	Annual layer (Straticounter)	✓
35.061	61	6	Annual layer (Straticounter)	✓
35.399	62	7	Annual layer (Straticounter)	✓
35.549	63	8	Annual layer (Straticounter)	✓

Table S2: Time markers used for the CP2025/1 timescale construction (part 2).

Depth in core #2 (m w.e.)	Age (yrsb2012)	Age uncertainty (years)	Type of time marker	Used in COPRA model
35.819	64	8	Annual layer (Straticounter)	✓
36.153	65	8	Annual layer (Straticounter)	✓
36.603	66	8	Annual layer (Straticounter)	✓
36.831	67	8	Annual layer (Straticounter)	✓
37.014	68	8	Annual layer (Straticounter)	✓
37.252	69	8	Annual layer (Straticounter)	✓
37.468	70	9	Annual layer (Straticounter)	✓
37.675	71	9	Annual layer (Straticounter)	✓
38.002	72	9	Annual layer (Straticounter)	✓
38.244	73	9	Annual layer (Straticounter)	✓
38.503	74	8	Annual layer (Straticounter)	✓
38.819	75	8	Annual layer (Straticounter)	✓
39.020	76	9	Annual layer (Straticounter)	✓
39.227	77	9	Annual layer (Straticounter)	✓
39.391	78	9	Annual layer (Straticounter)	✓
39.739	79	9	Annual layer (Straticounter)	✓
39.977	80	10	Annual layer (Straticounter)	✓
40.171	81	10	Annual layer (Straticounter)	✓
40.329	82	10	Annual layer (Straticounter)	✓
40.533	83	9	Annual layer (Straticounter)	✓
40.796	84	9	Annual layer (Straticounter)	✓
40.966	85	9	Annual layer (Straticounter)	✓
41.227	86	10	Annual layer (Straticounter)	✓
41.354	87	10	Annual layer (Straticounter)	✓
41.509	88	10	Annual layer (Straticounter)	✓
41.677	89	10	Annual layer (Straticounter)	✓
41.834	90	10	Annual layer (Straticounter)	✓
41.885	91	10	Annual layer (Straticounter)	✓
42.037	92	10	Annual layer (Straticounter)	✓
42.188	93	10	Annual layer (Straticounter)	✓
42.367	94	10	Annual layer (Straticounter)	✓
42.511	95	10	Annual layer (Straticounter)	✓
42.595	96	10	Annual layer (Straticounter)	✓
42.732	97	10	Annual layer (Straticounter)	✓
42.911	98	10	Annual layer (Straticounter)	✓
43.092	99	10	Annual layer (Straticounter)	✓
43.311	100	10	Annual layer (Straticounter)	✓
43.410	101	10	Annual layer (Straticounter)	✓
43.566	102	10	Annual layer (Straticounter)	✓
43.739	103	10	Annual layer (Straticounter)	✓
43.851	104	10	Annual layer (Straticounter)	✓
44.061	105	10	Annual layer (Straticounter)	✓
44.247	106	10	Annual layer (Straticounter)	✓
44.397	107	10	Annual layer (Straticounter)	✓
44.569	108	10	Annual layer (Straticounter)	✓
44.728	109	10	Annual layer (Straticounter)	✓
44.836	110	10	Annual layer (Straticounter)	✓
44.951	111	10	Annual layer (Straticounter)	✓
45.023	112	10	Annual layer (Straticounter)	✓
55.243	651	204	^{14}C of bulk (WIOC)	✓
58.433	1570	288	^{14}C of bulk (WIOC)	✓
58.850	2244	126	^{14}C of macrofragment	✓
59.470	2671	102	^{14}C of macrofragment	✓
60.288	4233	524	^{14}C of bulk (WIOC)	✓
60.510	5238	531	^{14}C of bulk (WIOC)	✓
60.712	6801	364	^{14}C of bulk (WIOC)	✓

Table S3: Time markers used for the and CP2025/2 timescale construction (part 1).

Depth in core #2 (m w.e.)	Age (yrsb2012)	Age uncertainty (years)	Type of time marker	Used in COPRA model
0.144	0.01	0.1	Annual layer (Straticounter)	✓
1.435	1	0.2	Annual layer (Straticounter)	✓
2.652	2	0.5	Annual layer (Straticounter)	✓
3.843	3	0.5	Annual layer (Straticounter)	✓
4.868	4	1	Annual layer (Straticounter)	✓
5.713	5	1	Annual layer (Straticounter)	✓
6.551	6	1	Annual layer (Straticounter) and 2006 pollen peak	✓
7.404	7	1	Annual layer (Straticounter)	✓
8.217	8	1	Annual layer (Straticounter)	✓
8.761	9	2	Annual layer (Straticounter)	✓
9.407	10	2	Annual layer (Straticounter)	✓
10.182	11	3	Annual layer (Straticounter)	✓
11.022	12	3	Annual layer (Straticounter)	✓
12.017	13	3	Annual layer (Straticounter)	✓
12.457	14	3	Annual layer (Straticounter)	✓
12.931	15	3	Annual layer (Straticounter)	✓
13.268	16	2	Annual layer (Straticounter)	✓
13.687	17	1	Annual layer (Straticounter) and 1995 pollen peak	✓
14.116	18	2	Annual layer (Straticounter)	✓
14.509	19	3	Annual layer (Straticounter)	✓
15.011	20	4	Annual layer (Straticounter)	✓
15.402	21	5	Annual layer (Straticounter)	✓
16.001	22	4	Annual layer (Straticounter)	✓
16.454	23	4	Annual layer (Straticounter)	✓
17.121	24	4	Annual layer (Straticounter)	✓
17.712	25	3	Annual layer (Straticounter)	✓
18.332	26	2	Annual layer (Straticounter) and 1986 Beta peak	✓
19.395	27	3	Annual layer (Straticounter)	✓
20.036	28	4	Annual layer (Straticounter)	✓
21.048	29	5	Annual layer (Straticounter)	✓
21.660	30	5	Annual layer (Straticounter)	✓
22.223	31	5	Annual layer (Straticounter)	✓
22.884	32	6	Annual layer (Straticounter)	✓
23.162	33	6	Annual layer (Straticounter)	✓
23.615	34	5	Annual layer (Straticounter)	✓
23.952	35	5	Annual layer (Straticounter)	✓
24.536	36	6	Annual layer (Straticounter)	✓
25.043	37	6	Annual layer (Straticounter)	✓
25.761	38	6	Annual layer (Straticounter)	✓
26.200	39	6	Annual layer (Straticounter)	✓
26.633	40	6	Annual layer (Straticounter)	✓
27.166	41	7	Annual layer (Straticounter)	✓
27.510	42	7	Annual layer (Straticounter)	✓
27.849	43	7	Annual layer (Straticounter)	✓
28.550	44	7	Annual layer (Straticounter)	✓
28.880	45	6	Annual layer (Straticounter)	✓
29.307	46	5	Annual layer (Straticounter)	✓
29.573	47	4	Annual layer (Straticounter)	✓
29.985	48	3	Annual layer (Straticounter)	✓
30.327	49	2	Annual layer (Straticounter) and 1963 tritium beta peaks	✓
30.802	50	3	Annual layer (Straticounter)	✓
31.295	51	4	Annual layer (Straticounter)	✓
31.599	52	5	Annual layer (Straticounter)	✓
31.966	53	6	Annual layer (Straticounter)	✓
32.334	54	5	Annual layer (Straticounter)	✓
32.775	55	4	Annual layer (Straticounter)	✓
33.118	56	3	Annual layer (Straticounter)	✓
33.496	57	2	Annual layer (Straticounter) and 1955 beta peak	✓
33.964	58	3	Annual layer (Straticounter)	✓
34.427	59	4	Annual layer (Straticounter)	✓
34.710	60	5	Annual layer (Straticounter)	✓
35.061	61	6	Annual layer (Straticounter)	✓
35.399	62	7	Annual layer (Straticounter)	✓
35.549	63	8	Annual layer (Straticounter)	✓

Table S3: Time markers used for the and CP2025/2 timescale construction (part 2).

Depth in core #2 (m w.e.)	Age (yrsb2012)	Age uncertainty (years)	Type of time marker	Used in COPRA model
35.819	64	8	Annual layer (Straticounter)	✓
36.153	65	8	Annual layer (Straticounter)	✓
36.603	66	8	Annual layer (Straticounter)	✓
36.831	67	8	Annual layer (Straticounter)	✓
37.014	68	8	Annual layer (Straticounter)	✓
37.252	69	8	Annual layer (Straticounter)	✓
37.468	70	9	Annual layer (Straticounter)	✓
37.675	71	9	Annual layer (Straticounter)	✓
38.002	72	9	Annual layer (Straticounter)	✓
38.244	73	9	Annual layer (Straticounter)	✓
38.503	74	8	Annual layer (Straticounter)	✓
38.819	75	8	Annual layer (Straticounter)	✓
39.020	76	9	Annual layer (Straticounter)	✓
39.227	77	9	Annual layer (Straticounter)	✓
39.391	78	9	Annual layer (Straticounter)	✓
39.739	79	9	Annual layer (Straticounter)	✓
39.977	80	10	Annual layer (Straticounter)	✓
40.171	81	10	Annual layer (Straticounter)	✓
40.329	82	10	Annual layer (Straticounter)	✓
40.533	83	9	Annual layer (Straticounter)	✓
40.796	84	9	Annual layer (Straticounter)	✓
40.966	85	9	Annual layer (Straticounter)	✓
41.227	86	10	Annual layer (Straticounter)	✓
41.354	87	10	Annual layer (Straticounter)	✓
41.509	88	10	Annual layer (Straticounter)	✓
41.677	89	10	Annual layer (Straticounter)	✓
41.834	90	10	Annual layer (Straticounter)	✓
41.885	91	10	Annual layer (Straticounter)	✓
42.037	92	10	Annual layer (Straticounter)	✓
42.188	93	10	Annual layer (Straticounter)	✓
42.367	94	10	Annual layer (Straticounter)	✓
42.511	95	10	Annual layer (Straticounter)	✓
42.595	96	10	Annual layer (Straticounter)	✓
42.732	97	10	Annual layer (Straticounter)	✓
42.911	98	10	Annual layer (Straticounter)	✓
43.092	99	10	Annual layer (Straticounter)	✓
43.311	100	10	Annual layer (Straticounter)	✓
43.410	101	10	Annual layer (Straticounter)	✓
43.566	102	10	Annual layer (Straticounter)	✓
43.739	103	10	Annual layer (Straticounter)	✓
43.851	104	10	Annual layer (Straticounter)	✓
44.061	105	10	Annual layer (Straticounter)	✓
44.247	106	10	Annual layer (Straticounter)	✓
44.397	107	10	Annual layer (Straticounter)	✓
44.569	108	10	Annual layer (Straticounter)	✓
44.728	109	10	Annual layer (Straticounter)	✓
44.836	110	10	Annual layer (Straticounter)	✓
44.951	111	10	Annual layer (Straticounter)	✓
45.023	112	10	Annual layer (Straticounter)	✓
49.332	257	20	Pb tie point with SZ core	✓
51.070	337	20	Pb tie point with SZ core	✓
51.568	387	20	Pb tie point with SZ core	✓
52.482	467	20	Pb tie point with SZ core	✓
54.652	717	40	Pb tie point with SZ core	✓
55.243	651	204	^{14}C of bulk (WIOC)	✗
56.203	1117	60	Pb tie point with SZ core	✓
57.045	1277	50	Pb tie point with SZ core	✓
58.110	1637	30	Pb tie point with SZ core	✓
58.295	1767	50	Pb tie point with SZ core	✓
58.433	1570	288	^{14}C of bulk (WIOC)	✗
58.850	2244	126	^{14}C of macrofragment	✗
58.994	2077	40	Pb tie point with SZ core	✓
59.107	2187	30	Pb tie point with SZ core	✓
59.470	2671	102	^{14}C of macrofragment	✓
60.288	4233	524	^{14}C of bulk (WIOC)	✓
60.510	5238	531	^{14}C of bulk (WIOC)	✓
60.712	6801	364	^{14}C of bulk (WIOC)	✓

Supplementary references

- Arienzo, M. M., McConnell, J. R., Chellman, N., and Kipfstuhl, S.: Method for Correcting Continuous Ice-Core Elemental Measurements for Under-Recovery, Environ. Sci. Technol., 53, 5887-5894, 10.1021/acs.est.9b00199, 2019.
- Avak, S., Schwikowski, M., Eichler, A.: Impact and implications of meltwater percolation on trace element records observed in a high-Alpine ice core.“ J. Glaciol. 64 (248): 877-886. doi:10.1017/jog.2018.74, 2018.
- Brugger, S. O., Schwikowski, M., Gobet, E., Schwörer, C., Rohr, C., Sigl, M., Henne, S., Pfister, C., Jenk, T. M., Henne, P. D., and Tinner, W.: Alpine Glacier Reveals Ecosystem Impacts of Europe's Prosperity and Peril Over the Last Millennium, Geoph. Res. Let., 48, e2021GL095039, https://doi.org/10.1029/2021GL095039, 2021.
- Cogley, J. G., Hock, R., Rasmussen, L. A., Arendt, A. A., Bauder, A., Braithwaite, R. J., Jansson, P., Kaser, G., Möller, M., Nicholson, L., and Zemp, M.: Glossary of glacier mass balance and related term, UNESCO/IHP, Paris2011.
- Festi, D., Carturan, L., Kofler, W., dalla Fontana, G., de Blasi, F., Cazorzi, F., Bucher, E., Mair, V., Gabrielli, P., and Oeggl, K.: Linking pollen deposition, snow accumulation on the Alto dell'Ortles glacier (South Tyrol, Italy) for sub-seasonal dating of a firn temperate core, The Cryosphere, 11, 937-948, 2017.
- Gabrieli, J.: Trace elements and Polycyclic Aromatic Hydrocarbons (PAHs) in snow and ice sampled at Colle Gnifetti, Monte Rosa (4450 m), during the last 10,000 years: environmental and climatic implication, PhD thesis, Department of Environmental Science, University of Venice, Venice, 178 pp., 2008.
- Gabrieli, J. and Barbante, C.: The Alps in the age of the Anthropocene: the impact of human activities on the cryosphere recorded in the Colle Gnifetti glacier, Rend. Fis. Acc. Lincei, 25, 71-83, 10.1007/s12210-014-0292-2, 2014.
- Gabrielli, P., Barbante, C., Bertagna, G., Bertó, M., Binder, D., Carton, A., Carturan, L., Cazorzi, F., Cozzi, G., Dalla Fontana, G., Davis, M., De Blasi, F., Dinale, R., Dragà, G., Dreossi, G., Festi, D., Frezzotti, M., Gabrieli, J., Galos, S., Ginot, P., Heidenwolf, P., Jenk, T. M., Kehrwald, N., Kenny, D., Magand, O., Mair, V., Mikhalenko, V. N., Lin, P. N., Oeggl, K., Piffer, G., Rinaldi, M., Schotterer, U., Schwikowski, M., Seppi, R., Spolaor, A., Stenni, B., Tonidandel, D., Uglietti, C., Zagorodnov, V. S., Zanoner, T., and Zennaro, P.: Age of the Mt. Ortles ice cores, the Tyrolean Iceman and glaciation of the highest summit of South Tyrol since the Northern Hemisphere Climatic Optimum, The Cryosphere, 10, 2779–2797, 10.5194/tc-10-2779-2016, 2016.
- Hill, M. O.: Correspondence Analysis: A Neglected Multivariate Method, Journal of the Royal Statistical Society Series C Royal Statistical Society, 23(3),340-354, 1974
- Huber, C.J., Eichler, A., Mattea, E., Brütsch, S., Jenk, T. M., Gabrieli, J., Barbante, C., Schwikowski M.: High-altitude glacier archives lost due to climate change-related melting. Nat. Geosci. 17, 110–113. https://doi.org/10.1038/s41561-023-01366-1, 2024.
- Jenk, T. M., Szidat, S., Bolius, D., Sigl, M., Gäggeler, H. W., Wacker, L., Ruff, M., Barbante, C., Boutron, C. F., and Schwikowski, M.: A novel radiocarbon dating technique applied to an ice core from the Alps indicating late Pleistocene ages J. Geophys. Res. Atmos., 114, 10.1029/2009JD011860, 2009.
- McConnell, J.R., Chellman, N.J., Plach, A., Wilson, A. I, Pan-European atmospheric lead pollution, enhanced blood lead levels, and cognitive decline from Roman-era mining and smelting, Proc. Natl. Acad. Sci., 122 (3) e2419630121, https://doi.org/10.1073/pnas.2419630121, 2025.
- Münster, T.S., Jenk, T.M., Eichler, A., Lee, G., and Schwikowski, M.: Performance of ICP-TOF-MS for ultra-trace element analyses in ice cores, J. Anal. Atom. Spectrom. https://doi.org/10.1039/D5JA00286A, 2025.
- Rhodes, R.H., Baker, J.A., Millet, M.A., and Bertler, A.N., Experimental investigation of the effects of mineral dust on the reproducibility and accuracy of ice core trace element analyses. Chem. Geol. 286 (3–4), 207–221. http://dx.doi.org/10.1016/chemgeo.2011.05.006, 2011.
- von Scheffer, C., De Vleeschouwer, F., Le Roux, G., Unkel, I.: Mineral dust and lead deposition from land use and metallurgy in a 4800-year-old peat record from the Central Alps (Tyrol, Austria), Quaternary International, 700-701, 68–79, 2024.

- Schwikowski, M., Barbante, C., Doering, T., Gaeggeler, H. W., Boutron, C. F., Schotterer, U., Tobler, L., Van de Velde, K., Ferrari, C., Cozzi, G., Rosman, K., and Cescon, P.: Post-17th-century changes of European lead emissions recorded in high-altitude alpine snow and ice, Environ. Sci. Technol., 38, 957-964, 2004.
- Sigl, M., Abram, N. J., Gabrieli, J., Jenk, T. M., Osmont, D., and Schwikowski, M.: 19th century glacier retreat in the Alps preceded the emergence of industrial black carbon deposition on high-alpine glaciers, The Cryosphere, 12, 3311-3331, 10.5194/tc-12-3311-2018, 2018.
- Sigl, M., Jenk, T. M., Kellerhals, T., Szidat, S., Gäggeler, H. W., Wacker, L., Synal, H. A., Boutron, C. F., Barbante, C., Gabrieli, J., and Schwikowski, M.: Intruments and methods: towards radiocarbon dating of ice cores, J. Glaciol., 55, 985-996, 2009.
- Uglietti, C., Gabrielli, P., Olesik, J. W., Lutton, A., and Thompson, L. G.: Large variability of trace element mass fractions determined by ICP-SFMS in ice core samples from worldwide high altitude glaciers, Appl. Geochem., 47, 109-121, 2014.
- Whillans, I. M.: The Equation of Continuity and its Application to the Ice Sheet Near “byrd” Station, Antarctica, J. Glaciol., 18, 359-371, 10.3189/S0022143000021055, 1977.